



Modification of metal organic framework HKUST-1 with CuCl for selective separation of CO/H₂ and CO/N₂

Yu Yin¹ · Zhi-Hao Wen¹ · Xiao-Qin Liu² · Lei Shi³ · Ai-Hua Yuan¹

© Springer Science+Business Media, LLC, part of Springer Nature 2018

Abstract

Separation and recovery of CO from CO, H₂, and N₂ mixtures is quite imperative, due to the huge demands in chemical industry, aims of human health, and regulations of hydrogen fuel cell techniques. Cu(I) π complexation adsorbents show great potentials for CO adsorption. In this work, the typical MOF, HKUST-1 was modified with CuCl by the monolayer dispersion method for preparation of π complexation adsorbents. The resultant adsorbents were well characterized with XRD, and N₂ adsorption–desorption isotherms (–196 °C). These results suggest that CuCl has been successfully modified on HKUST-1. The CO, H₂, and N₂ adsorption performance of the adsorbents at 25 °C was tested as well. In addition, CO/H₂ and CO/N₂ selectivity was predicted by the ideal adsorbed solution theory (IAST). In general, the adsorbents modified with CuCl show better performance than pristine HKUST-1 on the CO separation from CO, H₂, and N₂ mixtures, including the CO adsorption capacity and the CO/H₂, CO/N₂ selectivity.

Keywords π complexation · CO adsorption · CuCl · Selectivity · HKUST-1

1 Introduction

As the raw material for generation of methane, phosgene, acetic acid, formic acid, and dimethyl formamide, etc., carbon monoxide (CO) is in a large demand in chemical industry. In general, a large scale of CO is obtained from steam reforming, steel plants, partial oxidation of hydrocarbons, and other industrial processes. CO is no doubt a high-yield

source. However, other redundant gases such as H₂ and N₂ always generate together with CO. To make use of CO as the raw material for generation of chemical products, separation and recovery of CO from gas mixtures is quite imperative [1]. On the other side, CO has toxic effects on the human's tissues and cells. Inhalation of CO should cause undue shortness of breath, or even death [2]. Furthermore, as the impurity in the catalytic reaction of hydrogen fuel cells, residual CO is poisonous to the catalysts [3]. In short, separation and recovery of CO from gas mixtures is highly necessary for the purposes of protecting human health and improving catalytic efficiency.

Many studies so far have been focused on using the adsorption technology for gas separation, due to that the process could be performed on mild conditions with high efficiency [4–7]. Adsorbent has the key influence on the separation performance. In order to separate and recover CO with high purity from gas mixtures, the adsorbent should exhibit high capacity and selectivity. It is reported that the Cu(I) ion could form the π complexation bonds with C=O in the CO molecule, and the π complexation bonds are stronger than van der Waals forces [8, 9]. Thus, Cu(I) modified adsorbents show high capacity and selectivity for CO adsorption from CO, H₂, and N₂ mixtures. Recently, much attention has been paid to preparation of adsorbents modified

✉ Yu Yin
season_july@just.edu.cn

✉ Xiao-Qin Liu
liuxq@njtech.edu.cn

✉ Ai-Hua Yuan
aihua.yuan@just.edu.cn

¹ School of Environmental and Chemical Engineering, Jiangsu University of Science and Technology, Zhenjiang 212003, China

² State Key Laboratory of Materials-Oriented Chemical Engineering, College of Chemistry and Chemical Engineering, Nanjing Tech University, Nanjing 210009, China

³ State Key Laboratory of Lake Science and Environment, Nanjing Institute of Geography and Limnology, Chinese Academy of Sciences, Nanjing 210008, China

with the Cu(I) ion. For preparation of Cu(I) π complexation adsorbents, the porous materials with high surface areas are essential for the purpose of dispersion of the Cu(I) ion. So far, zeolites, active carbons, and mesoporous silicas, etc. are the most widely used inorganic porous materials to work as the supports. This application has been commercialized in the 1990s by Xie et al. [10], Golden et al. [11] and Nishida et al. [12]. They have designed and built the most commercial adsorbents using thermal dispersion of CuCl on NaY zeolite. Although commercialized, it is worth improving the efficiency to a higher level. Thus, Cu(I) modified porous materials attracts many researchers' attention as well. Gao et al. introduced CuCl into the Y zeolite for preparation of the CuCl/Y adsorbent [13]. Ma et al. loaded Cu(I) ions on the active carbon for achievement of the Cu(I)/AC adsorbent [14]. The authors previously incorporated Cu₂O into mesoporous silica SBA-15 for acquirement of the Cu₂O/SBA-15 adsorbent [15]. The π complexation adsorbents of CuCl/Y, Cu(I)/AC, and Cu₂O/SBA-15 were applied to the CO adsorption from gas mixtures. And the results demonstrate that the Cu(I) modified adsorbents show much higher adsorption capacity and selectivity than the supports. It is worthwhile mentioning that modification of the porous materials with the Cu(I) ion is an efficient method for preparation of π complexation adsorbents, which could show enhanced capacity and selectivity on CO adsorption from gas mixtures.

Metal Organic Frameworks (MOFs) are classified as inorganic–organic hybrid materials, and have received tremendous interests in catalysis [16, 17], adsorption [17–20], and drug release [21–23]. MOFs show superior properties such as super high surface areas and tunable pore structures, etc., which make them one of the most promising porous materials [24, 25]. Much work so far has been focused on the preparation of π complexation adsorbents by use of MOFs as the supports. However, the general applications of the obtained Cu(I) modified MOFs are dedicated to olefin/paraffin separation [26, 27] and desulfurization [28–30]. In rare cases, the application of MOFs as the supports for CO adsorption has been reported. To the best of our knowledge, there is only one report on the Cu(I) modified MOFs for CO adsorption up to now. Li and co-workers prepared the adsorbents by use of MIL-100(Fe) as the support [31]. The CuCl₂ precursor was firstly introduced to MIL-100(Fe), and then reduced to the Cu(I) ion. The resultant adsorbents show high CO adsorption capacity and CO/N₂ selectivity. One important future direction of MOFs is to work as the supports of π complexation adsorbents for their application on CO separation from gas mixtures.

In the present study, we use HKUST-1 (HKUST = Hong Kong University of Science and Technology) as the support for preparation of π complexation adsorbents for CO separation from gas mixtures, for the first time. HKUST-1

is a typical MOF, which is also named Cu₃(BTC)₂, (BTC = 1,3,5-benzenetricarboxylic acid). The π complexation adsorbents were prepared by direct modification of the Cu(I) ion on HKUST-1 through the monolayer dispersion method. CuCl is not priceless and easily acquired. Therefore, CuCl is a good choice of the cuprous source. The obtained adsorbents were denoted as CuHT, and were characterized with XRD, and N₂ adsorption–desorption isotherms (–196 °C). The combination states of CuCl and HKUST-1 were investigated. The results show that CuCl has been successfully modified on HKUST-1. We also demonstrate that the CuHT adsorbents show excellent performance for selective adsorption of CO from CO, H₂, and N₂ mixtures. Both the CO adsorption capacity and CO/H₂, CO/N₂ selectivity (IAST) of CuHT adsorbents are evidently better than that of pristine HKUST-1.

2 Experimental

2.1 Materials synthesis

2.1.1 HKUST-1

HKUST-1 was prepared according to the typical method. 2.077 g of Cu(NO₃)₂·3H₂O was dissolved in 15 mL of deionized water. 1.0 g of H₃BTC (H₃BTC = 1,3,5-benzenetricarboxylic acid) was dissolved in the mixed solvent consisting of DMF (15 mL) and ethanol (15 mL). The above solution was mixed together and transferred into a 50 mL Teflon-lined stainless steel autoclave, and then heated at 100 °C for 10 h. The as synthesized HKUST-1 was filtered, and washed with DMF for three times. To remove DMF in the pores, the sample was exchanged with dichloromethane twice in 3 days.

2.1.2 CuCl

The CuCl powder with partial oxidation should have a purification treatment before use. 3 g of the CuCl powder was dissolved in 10 mL of HCl (12 M). Then 100 mL of deionized water was added and stirred for generation of the white precipitate. The white precipitate was recovered by filtration under the protection of ethanol. After the hydrothermal treatment at 80 °C for 4 h under vacuum, purified CuCl powder was obtained.

2.1.3 xCuHT

The CuCl was incorporated on HKUST-1 by the monolayer dispersion method. It is a facile method for modification of porous materials with metal compounds [32, 33]. HKUST-1 was firstly activated at 120 °C for 12 h. The purified CuCl

and activated HKUST-1 were mixed by solid-state grinding at ambient conditions within 2 min. The mixture was then calcined in flowing argon at 200 °C for 2 h with a heating rate of 2 °C min⁻¹. The obtained samples were denoted as *x*CuHT. The content of CuCl in the *x*CuHT adsorbents is *x* wt%.

2.2 Materials characterization

X-ray diffraction (XRD) patterns of the materials were recorded on a Bruker D8 Advance diffractometer with Cu K α radiation in the 2θ range from 5° to 60° at 40 kV and 40 mA. The N₂ adsorption–desorption isotherms were measured by using a BELSORP-max system at –196 °C. Prior to analysis, the samples were evacuated at 120 °C for 12 h. The Brunauer–Emmett–Teller (BET) surface area was calculated at the relative pressure ranged from 0.05 to 0.20. The total pore volume was derived from the amount adsorbed at the relative pressure of about 0.99.

2.3 Gas adsorption test

The gas adsorption isotherms of CO, H₂, and N₂ were measured on Micromeritics ASAP 2020 at 25 °C. About 100 mg of the sample was outgassed at the temperature of 120 °C for 12 h prior to measurement.

The CuCl dispersion on the adsorbents was calculated with surface CuCl molecules divided by total CuCl molecules [11]. The surface CuCl molecules were obtained from the enhanced adsorption capacity of CuHT to HKUST-1 ($V_{(\text{CuHT})} - V_{(\text{HKUST-1})}$, mL g⁻¹) divided by molar volume of CO gas (22.4 mL mmol⁻¹). The total CuCl molecules were generated from loading amount (*x*% g·g⁻¹) divided by molar mass of CuCl (0.099 g mmol⁻¹).

2.4 CO/H₂ and CO/N₂ selectivity calculation on the adsorption isotherms

In the analysis of adsorption equilibrium, the adsorption of CO, H₂, and N₂ can be described well by the Double Langmuir model [34] as shown in Eq. 1.

$$q = q_c \frac{K_c P}{1 + K_c P} + q_i \frac{K_i P}{1 + K_i P} \quad (1)$$

where the subscripts *c* and *i* referring to the channels and intersections, respectively. The geometrical constraint gives rise to two different saturation amounts adsorbed in locations *c* and *i* and indicated by q_c and q_i . This description of adsorption equilibrium contains four parameters and their values are obtained from the experimental isotherm data by nonlinear regression.

Ideal adsorbed solution theory (IAST) is a well-known approach to predicting multi-component adsorption isotherms from experimental or simulation data for single-component adsorption [35, 36]. IAST is analogous to Raoult's law for vapor–liquid equilibrium as shown in Eq. 2.

$$P_i = P_i^o(\pi_i)x_i \quad (2)$$

where x_i and π_i are the molar fraction and spreading pressure of component *i* in the adsorbed phase, respectively. At the adsorption equilibrium, the reduced spreading pressures must be the same for each component and the mixture as depicted in Eqs. 3 and 4.

$$\pi_1^* = \pi_2^* = \dots = \pi_N^* \quad i = 1, 2, 3, \dots, N \quad (3)$$

$$\pi_i^* = \frac{\pi_i A}{RT} = \int_0^P \frac{q}{P} dp \quad (4)$$

where q is the pure component equilibrium capacity and P is the pure component hypothetical pressure which yields the same spreading pressure as that of the mixture.

The selectivity of CO over H₂ (N₂) on different adsorbents is calculated via Eq. 5.

$$S_{ij} = \frac{x_i/x_j}{y_i/y_j} \quad (5)$$

where x_i and x_j are the equilibrated adsorption capacity of CO and H₂ (N₂) respectively, and y_i and y_j are the molar fractions of CO and H₂ (N₂) in gas phases respectively.

2.5 Isothermic heat calculation on the adsorption isotherms at different temperatures

The gas adsorption isotherms of CO at 15 °C were measured as well in order to calculate the isosteric heat of adsorption, and the Clausius–Clapeyron equation (Eq. 6) was used.

$$\ln \frac{p_2}{p_1} = \frac{-\Delta H_S}{R} \left(\frac{1}{T_2} - \frac{1}{T_1} \right) \quad (6)$$

where ΔH_S is the isosteric heat of adsorption, p is the equilibrium pressure at the temperature T , and R is the universal gas constant. The partial pressure for different temperatures at fixed adsorption capacity can be calculated from the fitted Double Langmuir equations.

3 Results and discussion

3.1 Characterization of the adsorbents

Figure 1 provides the XRD patterns of HKUST-1 and CuCl modified samples. The diffraction peaks of the HKUST-1

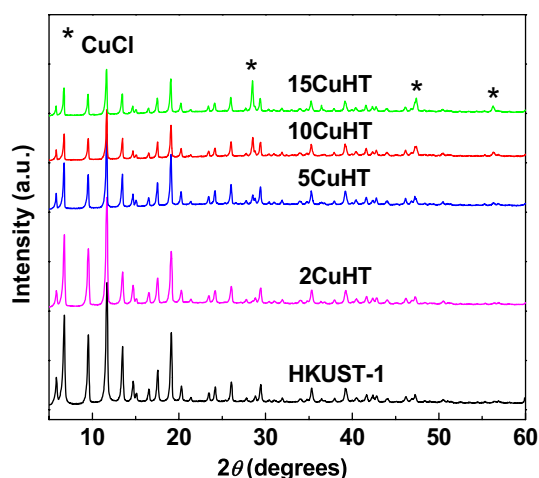


Fig. 1 Wide-angle XRD patterns for the samples of HKUST-1 and CuHT

sample match well with the simulated patterns calculated from the corresponding crystallographic data. This indicates that the synthesized HKUST-1 is phase-pure. With the modification of CuCl, the CuHT samples maintain the peaks of HKUST-1, suggesting the well preservation of crystalline characters of HKUST-1. The intensity of diffraction peaks of HKUST-1 decrease gradually with the increasing content of CuCl on the CuHT samples. This should be ascribed to the decreasing content of HKUST-1 in the CuHT samples. In addition, some new peaks at 2θ of 28.4° , 47.5° and 56.5° derived from CuCl (JCPDS no. 06-0344) appear on the CuHT samples. With the increase of CuCl content, the intensity of diffraction peaks of CuCl increases gradually. This confirms the successful modification of CuCl on the CuHT adsorbents.

Figure 2 displays the N_2 adsorption–desorption isotherms of the samples at -196°C . BET surface areas, and total pore

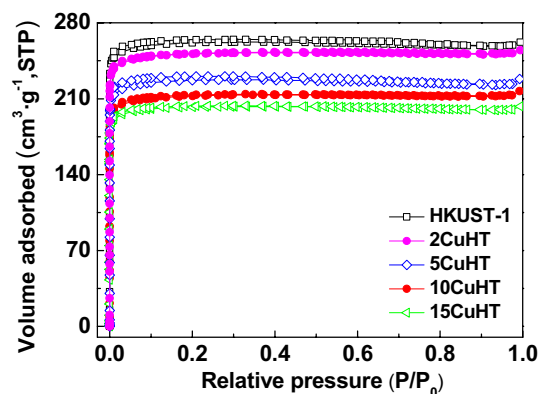


Fig. 2 N_2 adsorption–desorption isotherms of HKUST-1 and CuHT samples

volumes calculated according to the isotherms are listed in Table 1. The HKUST-1 and CuHT samples exhibit the similar isotherms, which show a rapid increase at low relative pressure followed by a platform. This is the characteristic of a typical type-I sorption, corresponding to the microporous structure. In comparison with the pristine HKUST-1, the CuCl modified samples have the lower N_2 adsorption capacity. Moreover, the adsorption capacity gradually decreases with the increase of the CuCl content. In addition, the pristine HKUST-1 displays the highest BET surface area of $1070\text{ m}^2\text{ g}^{-1}$ and a pore volume of $0.405\text{ cm}^3\text{ g}^{-1}$. After modification of HKUST-1 with gradually increasing content of CuCl, both the BET surface areas and pore volumes have regular changes. For the samples of CuHT with the CuCl content ranging from 2 to 15 wt%, the BET surface areas decline from 1014 to $816\text{ m}^2\text{ g}^{-1}$, and the pore volumes drop from 0.393 to $0.313\text{ cm}^3\text{ g}^{-1}$. It is reasonable to believe that CuCl modified on HKUST-1 is the primary cause of the decreasing BET surface areas and pore volumes.

Taken together of the XRD and N_2 adsorption–desorption results, firstly, we have evidenced that the microstructure of HKUST-1 is well maintained with the modification of CuCl. Secondly, the existence of CuCl in the CuHT samples is assured by the XRD patterns. Thirdly, the BET surface areas and pore volumes of the CuHT samples drop with the modification of CuCl. The results indicate the presence of CuCl supported on the HKUST-1 framework once again.

3.2 Adsorption performance of the adsorbents

The obtained HKUST-1 and CuHT adsorbents were applied to CO , H_2 and N_2 adsorption. The isotherms were fitted using Double Langmuir model and the CO/H_2 and CO/N_2 selectivity was calculated as well. Figure 3 depicts the CO adsorption isotherms for the samples at 25°C . The pristine HKUST-1 shows the worst performance and is capable of $7.2\text{ cm}^3\text{ g}^{-1}$ of CO at 100 kPa . The modification of CuCl on HKUST-1 improves the CO adsorption capacity evidently. For the CuCl modified samples, the amount of CO captured at 100 kPa steps up from 8.3 to $13.4\text{ cm}^3\text{ g}^{-1}$ with the increase of CuCl content from 2 to 10 wt%. Then a further increase in CuCl content up to 15 wt% results in the CO adsorption capacity decline back to $10.5\text{ cm}^3\text{ g}^{-1}$. The results

Table 1 Physicochemical properties of HKUST-1 and CuHT samples

Sample	S_{BET} ($\text{m}^2\text{ g}^{-1}$)	V_p ($\text{cm}^3\text{ g}^{-1}$)	Dispersion (%)
HKUST-1	1070	0.405	–
2CuHT	1014	0.393	22.8
5CuHT	914	0.352	16.4
10CuHT	855	0.335	27.0
15CuHT	816	0.313	6.6

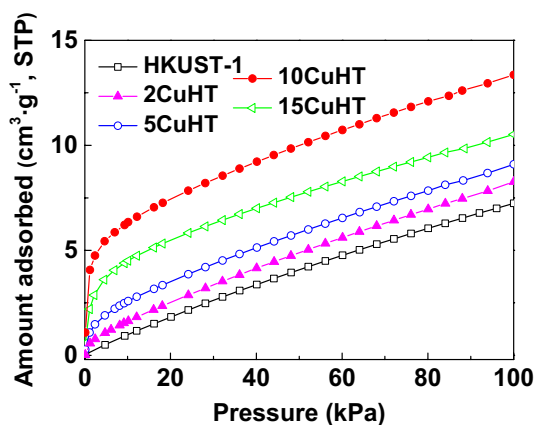


Fig. 3 CO adsorption isotherms for the samples of HKUST-1 and CuHT at 25 °C

of CuCl dispersion calculated according to the CO isotherms exhibit in Table 1. The results show that the dispersion of CuCl are 22.8, 16.4, 27.0 and 6.6% for 2CuHT, 5CuHT, 10CuHT and 15CuHT, respectively. It should be noted that the Cu(I) ion could form π complexation interactions with the C=O bond in the CO molecule. Thus, the increasing CuCl content in the 2CuHT, 5CuHT, and 10CuHT samples is the main reason for the improving capacity. However, the decreasing surface areas should make a compromise of the π complexation adsorption performance. This is the reason that the CO adsorption capacity of the 15CuHT sample no longer improves.

Fig. 4 Adsorption isotherms of CO, H₂, and N₂ on HKUST-1 and 10CuHT samples at 25 °C

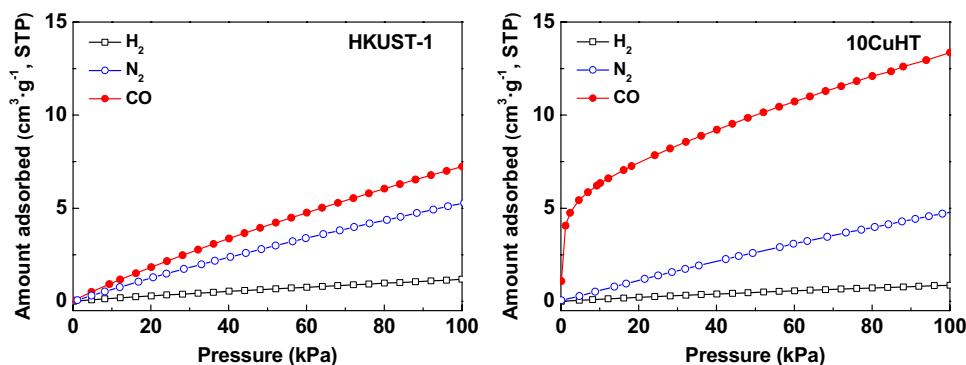


Table 2 Fitting parameters derived from isothermal data at 25 °C

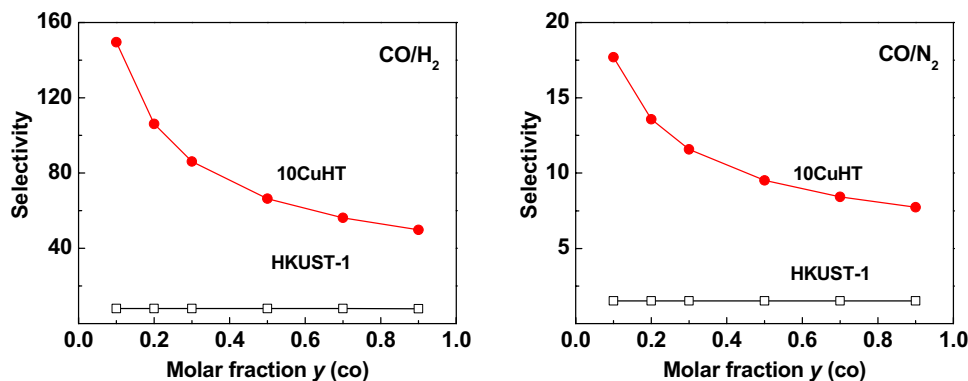
Adsorbent	Adsorbate	q_c (cm ³ g ⁻¹)	k_c (kPa ⁻¹)	q_i (cm ³ g ⁻¹)	k_i (kPa ⁻¹)	R ²
10CuHT	CO	4.05717	0.92533	26.44464	0.00324	0.9998
	H ₂	0.37174	0.01388	53.90168	0.00012	0.9999
	N ₂	6.61967	0.00096	21.60457	0.00241	0.9999
HKUST-1	CO	0.28779	0.11442	39.11310	0.00217	0.9999
	H ₂	0.11287	0.07181	43.87114	0.00025	0.9995
	N ₂	7.91449	0.00089	23.26125	0.00247	0.9999
15CuHT	CO	5.0605	0.96820	21.85553	0.00410	0.9997

Figure 4 profiles the adsorption isotherms of CO, H₂, and N₂ on HKUST-1 and 10CuHT samples. For the HKUST-1 sample, the adsorption uptake is 1.2 cm³ g⁻¹ for H₂, 5.3 cm³ g⁻¹ for N₂, and 7.2 cm³ g⁻¹ for CO. It is worth noting that, on the 10CuHT sample, the adsorption amount of CO goes up to 13.4 cm³ g⁻¹, whereas the adsorption capacity of H₂ and N₂ has a slight decline to 0.9 and 4.8 cm³ g⁻¹, respectively. Next, we should identify that the isotherm of CO adsorption for the 10CuHT sample shows a significant increase at low pressure. This is a typical type-I isotherm, which indicates that there is a strong interaction between 10CuHT and CO. The strong interaction is ascribed to the modified CuCl, which forms the π complexation bonds with CO. When it comes to H₂ and N₂ adsorption for the 10CuHT sample, the adsorption equilibrium isotherms are linear with the pressure. Besides, for the pristine HKUST-1, the adsorption equilibrium isotherms for CO, H₂, and N₂ are linear as well. The linear isotherms indicate the physical adsorption bonds between the adsorbents and gases.

To further predict the adsorption performance of the adsorbents in gas mixtures, the ideal adsorbed solution theory (IAST) method was used to evaluate the CO/H₂ and CO/N₂ selectivity at 100 kPa. The fitting parameters are listed in Tables 2 and 3, and the selectivity results are presented in Fig. 5. In a word, the selectivity of CO over the H₂ and N₂ gases on the 10CuHT sample is obviously higher than that on pristine HKUST-1, despite different molar fractions of CO in the gas mixtures. In more detail, the CO/H₂ selectivity is 8.0 on HKUST-1 at a CO molar fraction of 0.1,

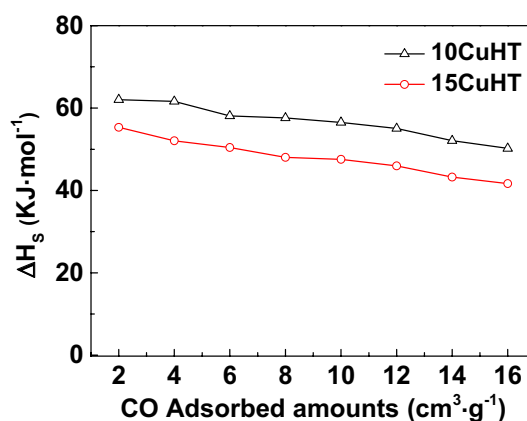
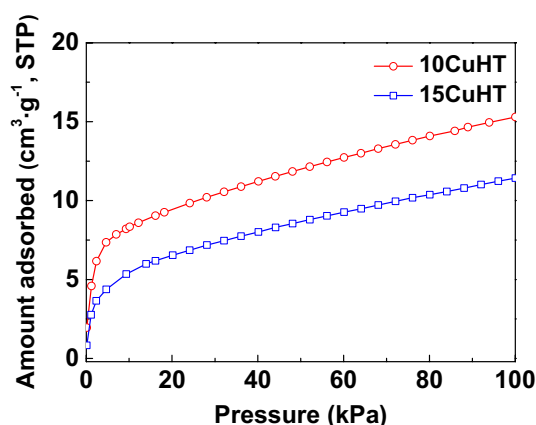
Table 3 Fitting parameters derived from isothermal data at 15 °C

Adsorbent	Adsorbate	q_c (cm ³ g ⁻¹)	k_c (kPa ⁻¹)	q_i (cm ³ g ⁻¹)	k_i (kPa ⁻¹)	R ²
10CuHT	CO	7.84478	1.38684	30.63474	0.00324	0.9988
15CuHT	CO	5.59193	1.83308	28.87942	0.00366	0.99995

Fig. 5 Selectivity profiles of CO/H₂ and CO/N₂ on HKUST-1 and 10CuHT at 100 kPa

while a higher selectivity of 149.5 is obtained on 10CuHT. Similarly, the selectivity of CO/N₂ can reach as high as 17.7 on 10CuHT, which is clearly larger than the value of 1.5 on HKUST-1. Thus, at current time, we should demonstrate that the CO/H₂ and CO/N₂ selectivity of 10CuHT is over 18 and 10 times larger than that of HKUST-1, respectively.

It is worth noting that the CuHT samples show better performance than pristine HKUST-1 on the CO separation from CO, H₂, and N₂ mixtures, including the CO adsorption capacity and the CO/H₂, CO/N₂ selectivity. It is inferred that the modified CuCl sites in the CuHT samples give rise to the enhanced performance. It is widely reported that the Cu(I) ion could form the π complexation bonds with C=O in the CO molecule [8, 13, 15, 31]. Besides, the π complexation bonds are stronger than van der Waals forces. Thus, the Cu(I) π complexation adsorbents show superior CO adsorption performance rather than H₂ and N₂. Herein, from the point of view of results, the adsorption isotherm of the pristine HKUST-1 for CO is linear, which corresponds to the van der Waals forces of HKUST-1 with CO. With regard to CuHT, the adsorption isotherm shows a significant increase at low pressure. This indicates that there is a strong interaction between CuHT and CO. In addition, the strong interaction is the π complexation bonds between the Cu(I) ion and C=O in the CO molecule. The isosteric heat of adsorption (Fig. 6) derived from the adsorption isotherms at 15 °C (Fig. 7) and 25 °C for the 10CuHT and 15CuHT samples are in the range of 40 to 65 KJ mol⁻¹. This value exceeds that of van der Waals forces, which confirms the strong interaction between CuHT and CO molecule. Besides, compared with 15CuHT, the 10CuHT sample with higher CuCl dispersion shows higher isosteric heat of adsorption. It reveals that high CuCl dispersion is helpful to make the surface force field toward CO more homogeneous. In general, the enhanced

**Fig. 6** Isosteric heat of adsorption for 10CuHT and 15CuHT samples**Fig. 7** Adsorption isotherms of CO for 10CuHT and 15CuHT samples at 15 °C

performance for the CuHT samples on CO adsorption is attributed to the incorporated Cu(I) ion, which form the π complexation bonds with CO.

4 Conclusions

In summary, the Cu(I) π complexation ion has been successfully modified on HKUST-1. The obtained CuHT adsorbents show better performance than pristine HKUST-1 on the CO adsorption from CO, H₂, and N₂ mixtures, including the CO adsorption capacity and the CO/H₂, CO/N₂ selectivity. Our results recently show that MOFs are the ideal candidates for preparing π complexation adsorbents, and there is a great potential to develop new Cu(I) modified MOFs for CO adsorption with enhanced capacity and selectivity.

Acknowledgements This work was supported by National Natural Science Foundation of China (51602133), Natural Science Foundation of Jiangsu Province (BK20160555), China Postdoctoral Science Foundation (2015M581750), Jiangsu Planned Projects for Postdoctoral Research Funds (1501114B), Qing Lan Project of Jiangsu Province, State Key Laboratory of Materials-Oriented Chemical Engineering (KL15-13).

References

1. D. Saha, S. Deng, *J. Chem. Eng. Data* **54**, 2245 (2009)
2. L. Wang, J.J. Zhao, L.L. Wang, T.Y. Yan, Y.Y. Sun, S.B.B. Zhang, *Phys. Chem. Chem. Phys.* **13**, 21126 (2011)
3. Y. Huang, Y. Tao, L. He, Y. Duan, J. Xiao, Z. Li, *Adsorption* **21**, 373 (2015)
4. S.J. Geier, J.A. Mason, E.D. Bloch, W.L. Queen, M.R. Hudson, C.M. Brown, J.R. Long, *Chem. Sci.* **4**, 2054 (2013)
5. Y.B. He, R. Krishna, B.L. Chen, *Energy Environ. Sci.* **5**, 9107 (2012)
6. Y. Yin, J. Zhu, X.Q. Liu, P. Tan, D.M. Xue, Z.M. Xing, L.B. Sun, *Rsc Adv.* **6**, 70446 (2016)
7. V.F.D. Martins, A.M. Ribeiro, A. Ferreira, U.H. Lee, Y.K. Hwang, J.S. Chang, J.M. Loureiro, A.E. Rodrigues, *Sep. Purif. Technol.* **149**, 445 (2015)
8. H.Y. Huang, J. Padin, R.T. Yang, *Ind. Eng. Chem. Res.* **38**, 2720 (1999)
9. F. Gao, Y.Q. Wang, X. Wang, S.H. Wang, *Rsc Adv.* **6**, 34439 (2016)
10. Y. Xie, N. Bu, J. Liu, G. Yang, J. Qiu, N. Yang, Y. Tang, *US* 4917711, (1990)
11. T.C. Golden, W.C. Kratz, F.C. Wilhelm, R. Pierantozzi, A. Rokicki, *US* 5258571, (1993)
12. T. Nishida, K. Tajima, Y. Osada, O. Shigyo, H. Taniguchi, *US* 4743276, (1988)
13. F. Gao, Y.Q. Wang, S.H. Wang, *Chem. Eng. J.* **290**, 418 (2016)
14. J.H. Ma, L. Li, J. Ren, R.F. Li, *Sep. Purif. Technol.* **76**, 89 (2010)
15. Y. Yin, P. Tan, X.Q. Liu, J. Zhu, L.B. Sun, *J. Mater. Chem. A.* **2**, 3399 (2014)
16. H. Furukawa, K.E. Cordova, M. O'Keeffe, O.M. Yaghi, *Science.* **341**, 974 (2013)
17. L.Q. Ma, C. Abney, W.B. Lin, *Chem. Soc. Rev.* **38**, 1248 (2009)
18. A. Cadiau, K. Adil, P.M. Bhatt, Y. Belmabkhout, M. Eddaoudi, *Science.* **353**, 137 (2016)
19. X.L. Cui, K.J. Chen, H.B. Xing, Q.W. Yang, R. Krishna, Z.B. Bao, H. Wu, W. Zhou, X.L. Dong, Y. Han, B. Li, Q.L. Ren, M.J. Zaworotko, B.L. Chen, *Science.* **353**, 141 (2016)
20. J. Zhang, X.Q. Liu, H. Zhou, X.F. Yan, Y.J. Liu, A.H. Yuan, *Rsc Adv.* **4**, 28908 (2014)
21. R. Ananthoji, J.F. Eubank, F. Nouar, H. Moultaki, M. Eddaoudi, J.P. Harmon, *J. Mater. Chem.* **21**, 9587 (2011)
22. J. Della Rocca, D.M. Liu, W.B. Lin, *Acc. Chem. Res.* **44**, 957 (2011)
23. X. Shen, B. Yan, *Dalton Trans.* **44**, 1875 (2015)
24. J.R. Long, O.M. Yaghi, *Chem. Soc. Rev.* **38**, 1213 (2009)
25. T. Uemura, N. Yanai, S. Kitagawa, *Chem. Soc. Rev.* **38**, 1228 (2009)
26. G.G. Chang, Z.B. Bao, Q.L. Ren, S.G. Deng, Z.G. Zhang, B.G. Su, H.B. Xing, Y.W. Yang, *Rsc Adv.* **4**, 20230 (2014)
27. Y.M. Zhang, B.Y. Li, R. Krishna, Z.L. Wu, D.X. Ma, Z. Shi, T. Pham, K. Forrest, B. Space, S.Q. Ma, *Chem. Commun.* **51**, 2714 (2015)
28. I. Ahmed, S.H. Jung, *Chem. Eng. J.* **251**, 35 (2014)
29. J.X. Qin, P. Tan, Y. Jiang, X.Q. Liu, Q.X. He, L.B. Sun, *Green Chem.* **18**, 3210 (2016)
30. N.A. Khan, S.H. Jung, *Angew. Chem. Int. Ed.* **51**, 1198 (2012)
31. J.J. Peng, S.K. Xian, J. Xiao, Y. Huang, Q.B. Xia, H.H. Wang, Z. Li, *Chem. Eng. J.* **270**, 282 (2015)
32. Y.C. Xie, Y.Q. Tang, *Adv. Catal.* **37**, 1 (1990)
33. Y. Yin, Z.F. Yang, Z.H. Wen, A.H. Yuan, X.Q. Liu, Z.Z. Zhang, H. Zhou, *Sci. Rep.* **7**, 4509 (2017)
34. W. Zhu, J.M. van de Graaf, L.J.P. van den Broeke, F. Kapteijn, J.A. Moulijn, *Ind. Eng. Chem. Res.* **37**, 1934 (1998)
35. J. Chen, L.S. Loo, K. Wang, *J. Chem. Eng. Data* **56**, 1209 (2011)
36. Z. Zhang, Z. Li, J. Li, *Langmuir.* **28**, 12122 (2012)